Journal of Zhejiang University-SCIENCE B 2025 26(11):1086-1102
www.jzus.zju.edu.cn; www.springer.com/journal/11585
E-mail: jzus_b@zju.edu.cn

Research Article
https://doi.org/10.1631/jzus.B2400235

Check for updates

Therapeutic effect of baicalein as an antiparasitic agent against *Toxoplasma gondii* in vitro and in vivo

Songrui WU[1,5*], Yingmei LAI[1*], Zhong'ao ZHANG[1], Jianzu DING[1,2,3], Shaohong LU[1,2,3], Huayue YE[4✉], Haojie DING[1,2,3✉], Xunhui ZHUO[1,2,3✉]

[1]*School of Basic Medical Sciences and Forensic Medicine, Hangzhou Medical College, Hangzhou 310013, China*
[2]*Engineering Research Center of Novel Vaccine of Zhejiang Province, Hangzhou Medical College, Hangzhou 310000, China*
[3]*Key Laboratory of Bio-tech Vaccine of Zhejiang Province, Hangzhou Medical College, Hangzhou 310000, China*
[4]*GuoTai (Taizhou) Center of Technology Innovation for Veterinary Biologicals, Taizhou 318000, China*
[5]*Health and Health Commission of Zigong City, Zigong 643000, China*

Abstract: The most common medications for the treatment of zoonotic toxoplasmosis are pyrimethamine and sulfadiazine, which may cause serious undesirable side effects. Thus, there is an urgent need to develop novel therapeutics. Baicalein (BAI, $C_{15}H_{10}O_5$) has been shown to perform well against protozoan parasites including *Leishmania* and *Cryptosporidium*. In this study, the inhibition efficacy of BAI on *Toxoplasma gondii* was evaluated using plaque, invasion, and intracellular proliferation assays. BAI effectively inhibited *T. gondii* (half-maximum inhibitory concentration (IC_{50})=6.457×10^{-5} mol/L), with a reduced invasion rate (33.56%) and intracellular proliferation, and exhibited low cytotoxicity (half-maximum toxicity concentration (TC_{50})= 5.929×10^{-4} mol/L). Further investigation using a mouse model shed light on the inhibitory efficacy of BAI against *T. gondii*, as well as the potential mechanisms underlying its anti-parasitic effects. The survival time of *T. gondii*-infected ICR mice treated with BAI was remarkably extended, and their parasite burdens in the liver and spleen were greatly reduced compared with those of the negative control group. Histopathological examination of live sections revealed effective therapeutic outcomes in the treatment groups, with no notable pathological alterations observed. Furthermore, alterations in cytokine levels indicated that BAI not only effectively suppressed the growth of *T. gondii* but also prevented excessive inflammation in mice. Collectively, these findings underscore the significant inhibitory efficacy of BAI against *T. gondii*, positioning it as a promising alternative therapeutic agent for toxoplasmosis.

Key words: *Toxoplasma gondii*; Baicalein (BAI); Antiparasitic; Immunity regulation

1 Introduction

Toxoplasma gondii is an obligate intracellular protozoan parasite that can infect a wide range of warm-blooded animals, including humans. The parasite has a complex life cycle that involves both sexual and asexual reproductive stages, and can form bradyzoites, which can persist in the host for long periods. The main routes of transmission include ingestion of contaminated food or water, consumption of raw or undercooked meat from infected animals, and vertical transmission from an infected mother to her fetus. In humans, *T. gondii* can cause a wide spectrum of clinical manifestations, ranging from asymptomatic or mild symptoms to severe and life-threatening diseases, particularly in immunosuppressed individuals or congenitally infected infants (Porter and Sande, 1992; Munoz et al., 2011; Daher et al., 2021).

Currently, the most common medications for the treatment of toxoplasmosis are pyrimethamine and sulfadiazine. However, both medications can cause some significant undesirable side effects, including bone marrow suppression, hematologic toxicity, and rash (Haverkos 1987; Porter and Sande 1992; Munoz et al., 2011). Moreover, prolonged use of these drugs

✉ Xunhui ZHUO, xhzhuo@gmail.com
Haojie DING, hjding@zjams.com.cn
Huayue YE, huayue_ye@126.com
* The two authors contributed equally to this work
Xunhui ZHUO, https://orcid.org/0000-0001-5805-0711
Huayue YE, https://orcid.org/0009-0007-2504-2652
Haojie DING, https://orcid.org/0009-0005-8263-8116

Received May 7, 2024; Revision accepted Oct. 12, 2024;
Crosschecked Sept. 29, 2025; Published online Oct. 25, 2025

can also lead to drug resistance or treatment failure. The therapeutic effects of alternative therapies, including pyrimethamine in combination with clindamycin, atovaquone, clarithromycin, or azithromycin, and monotherapy with trimethoprim sulfamethoxazole (TMP-SMX) or atovaquone are not superior to pyrimethamine or sulfadiazine (Kovacs, 1992; Porter and Sande, 1992; Fichera et al., 1995; Djurković-Djaković et al., 2002; Soheilian et al., 2011). Therefore, there is increasing interest in developing new drugs with better efficacy and safety profiles. At the same time, natural plant ingredients, especially those used in traditional Chinese medicine, have exhibited outstanding performance against *T. gondii* (Montazeri et al., 2017; Cheraghipour et al., 2021). These herb extracts, including flavonoids from *Phlomis nissolii* and *Hypericum perforatum*, are often found to be anti-inflammatory, antioxidant, and resistant to other parasites (Cheraghipour et al., 2021). Both baicalein (BAI) and baicalin (BC) are active ingredients from *Scutellaria baicalensis*. BAI is a flavonoid with strong antioxidant and anti-inflammatory effects and has been reported to have a variety of biological activities, including antibacterial, antiviral, antitumor, anti-cardiovascular, and neuroprotective effects (de Oliveira et al., 2015; Dinda et al., 2017; Luo et al., 2017; Sowndhararajan et al., 2017; Jin et al., 2019). BAI is also believed to have antidepressant and anxiolytic effects and may play a potential role in the treatment of certain skin diseases (Yun et al., 2010; Zhao et al., 2021). The main pharmacological effects of BC, a glycoside compound, are anti-inflammatory and antioxidant effects. Clinical studies have shown that BC can improve the condition of a variety of inflammatory diseases, including hepatitis, cholecystitis, dermatitis, allergic diseases, and tumors (Liu et al., 2014; Dinda et al., 2017; Liang et al., 2017; Hu et al., 2021; Wang et al., 2022). BC also has an antioxidant effect, reducing cell damage caused by free radicals, and BC has a protective effect against chronic diseases such as cardiovascular disease (Xin et al., 2020). BAI and BC have been widely used in traditional Chinese medicine preparations, nutraceuticals, and medical applications. Therefore, it is worth evaluating the antiparasitic effects of BAI and BC, particularly against protozoa, including *T. gondii*.

In this study, the anti-*T. gondii* effects of BAI and BC were evaluated both in vitro and in vivo. The findings indicate that BAI exerts a pronounced inhibitory effect on both the invasion and intracellular proliferation of *T. gondii*, leading to diminished in vivo damage, showing its great potential for application as an anti-*T. gondii* drug.

2 Materials and methods

2.1 Animals, cells, and *T. gondii* strain resource

Six- to eight-week-old female ICR mice were obtained from the Zhejiang Experimental Animal Centre and were housed under standard specific pathogen-free conditions. Human foreskin fibroblast (HFF) cells were obtained from the American Type Culture Collection (ATCC, Manassas, USA) and cultured in Dulbecco's modified Eagle's medium (DMEM; Gibco, USA) supplemented with 10% (volume fraction) fetal bovine serum (FBS; Gibco) and 1% (volume fraction) penicillin-streptomycin solution (Cienry, China). The cells were maintained at 37 ℃ in a humidified atmosphere containing 5% CO_2. The Rockefeller hospital (RH) strain of *T. gondii*, which was kept in our laboratory, was propagated and passaged in HFF cells under the same conditions.

2.2 Cytotoxicity assays

HFF cells were cultured in 96-well plates at a density of 2×10^4 cells per well in DMEM supplemented with 10% FBS at 37 ℃ and 5% CO_2 for 24 h to form a monolayer. The monolayers were then incubated with different concentrations (4×10^{-4}, 2×10^{-4}, 1×10^{-4}, 5×10^{-5}, and 2.5×10^{-5} mol/L) of BAI ($C_{15}H_{10}O_5$, Sigma-Aldrich, St. Louis, USA) or BC (Shanghai Yuanye Bio-Technology, China) for 48 h. HFF cells cultured in DMEM without any treatment served as the negative control (NC). All wells were washed twice with 200 μL of 10 mmol/L phosphate-buffered saline (PBS) solution, followed by the addition of 200 μL of fresh DMEM and 10 μL of cell counting kit-8 (CCK-8) reagents (Solarbio, China), and the cells were incubated for 1 h at 37 ℃. After incubation, the absorbance of each well was measured at 450 nm using a microplate reader (Thermo Fisher Scientific, USA). The experiment was performed in triplicate and repeated three times to obtain reliable results. The half-maximum toxicity concentration (TC_{50}) values of BAI and BC for the host cells were calculated as previously described by Zhang et al. (2019).

2.3 In vitro assessment of anti-*T. gondii* efficacy

As described above, HFF cells were cultured in 96-well plates for 24 h to obtain a monolayer of cells. Subsequently, cells were incubated with fresh tachyzoites of *T. gondii* RH strain at a multiplicity of infection (MOI) of 5:2 per well for 3 h at 37 ℃ and 5% CO_2. BAI and BC were half-diluted from 400 to 3.125 μmol/L and 100 to 12.5 μmol/L, respectively. After washing twice with 200 μL of PBS, the cultured medium of each well was replaced with fresh DMEM containing the above diluted BAI or BC. The cells were incubated for 48 h. After washing twice with 200 μL of PBS, the mixture containing 200 μL of fresh DMEM and 10 μL of CCK-8 reagent was added and incubated with the cells at 37 ℃ for 1 h. After incubation, the absorbance of each well was measured at 450 nm using a microplate reader. HFF cells cultured in fresh DMEM were used as the blank controls. The experiment was performed with five replicates and repeated twice. The half-maximum inhibitory concentration (IC_{50}) values of BAI and BC were calculated as described by Jiang et al. (2022).

2.4 Plaque assay

The plaque assay was performed as previously described (Fox and Bzik, 2002). A monolayer of HFF cells was cultured with 2 mL of DMEM containing either 65 μmol/L of BAI (the BAI group) or 400 μmol/L of sulfadiazine (SDZ) (the positive group), while HFF monolayers infected with 500 tachyzoites were regarded as the negative control (NC), and HFF cells without any treatment were regarded as the blank control. A total of 500 fresh extracellular RH tachyzoites were used to infect HFF cells in a 6-well cell culture plate for 7 d. After being washed three times with ice-cold PBS solution to remove extracellular RH tachyzoites, the HFF cells were fixed with methanol for 15 min and stained with 1.5% (volume fraction) crystalline violet for 30 min. The plaque area in each well was measured using ImageJ (National Institutes of Health, USA), and the proliferation of *T. gondii* was analyzed.

2.5 Invasion assay

The invasion assay was performed as described previously (Li et al., 2022). HFF cell monolayers were treated with DMEM containing an optimum concentration of BAI (resulting from a value of Section 2.4) for 8 h. HFF cells treated with 400 μmol/L of SDZ or without any drug were included as the positive control or NC, respectively. Then, HFF cells were infected with 1×10^7 RH tachyzoites for 30 min. The culture was gently removed, and the cells were washed three times with ice-cold PBS solution and fixed with 4% (0.04 g/mL) paraformaldehyde (PFA) for 30 min at room temperature. Cells were blocked with 1% (0.01 g/mL) bovine serum albumin (BSA) in PBS solution (1% BSA/PBS, volume fraction) overnight at 4 ℃. After washing three times with PBS solution, the cells were treated with a 1:50 (volume ratio) dilution of mouse anti-EPA45 antibody and incubated for 3 h at room temperature. After washing three times, goat anti-mouse Alexa Fluor 647 antibody (1:1000, volume ratio, the same below) was added, followed by incubation for 1 h in the dark. The cells were then permeabilized with 0.15% (volume fraction) Triton-X100 in PBS for 30 min. After three washes, the cells were again blocked with 1% BSA/PBS for 1 h at 37 ℃. Subsequently, the cells were incubated with rabbit anti-*T. gondii* granule antigen 7 (GRA7, 1:100) for 3 h. The goat anti-rabbit Alexa Fluor 488 antibody (1:1000) was then used as secondary antibody and incubated for 1 h in the dark. HFF cells and RH tachyzoites were then stained with 4',6-diamidino-2-phenylindole (DAPI; Beyotime Biotechnology, China) at room temperature for 30 min and observed using a fluorescence microscope (Olympus IX71, Tokyo, Japan). The color of intracellular parasites under the fluorescence microscope was green, and the color of extracellular parasites was yellow. The proportion of intracellular RH tachyzoites to the total number of RH tachyzoites was regarded as the invasion rate. Ten randomly selected fields of view were counted under the fluorescence microscope, and the experiment was repeated three times.

2.6 Intracellular proliferation assay

To assess the replication rate of *T. gondii* in HFF cells, the HFF cells in 28-mm glass-bottomed dishes were infected with 1×10^6 RH tachyzoites for 30 min, followed by washing with PBS and incubation for 48 h. After washing, the cells were fixed with 4% PFA at room temperature for 30 min. Additionally, cells were permeabilized with 0.15% Triton-X100 in PBS solution for 30 min, and then blocked with 1% BSA/PBS at 4 ℃ overnight. Subsequently, cells were

incubated with rabbit anti-*T. gondii* GRA7 antibody (1:100) for 3 h, followed by goat anti-rabbit Alexa Fluor 488 antibody (1:1000) for 1 h in the dark and then stained with DAPI for 5 min. The replication of RH tachyzoites within cells was analyzed by observing at least 100 vacuoles through fluorescence microscopy and categorizing the vacuoles as 1, 2, 4, 8, 16, or >16, with three independent replicates for each count.

2.7 Evaluation of BAI's anti-*T. gondii* activity in vivo

A total of 50 female ICR mice were divided equally into five groups, and 40 mice were injected intraperitoneally (i.p.) with 1×10^3 tachyzoites of *T. gondii* RH strain for drug treatment. Mice administered intragastrically (i.g.) with 100 or 75 mg/kg of BAI were assigned to the high-dose BAI treatment group (BH) or medium-dose BAI treatment group (BM), respectively. Mice treated with 100 mg/kg of SDZ were included as the SDZ-positive group, and those treated with PBS solution as the NC. The mice without any treatment served as the blank control group. After infection for 3 h, treatments were administered accordingly once a day for 14 d. Survival analysis was performed up to 30 d. The peritoneal fluids of mice were collected for parasite burden analysis to determine the proliferation level of *T. gondii*.

2.8 Parasite burden in mouse tissues and ascites

As previously described (Liu et al., 2020), the liver and spleen tissues of the mice were separately isolated and mixed in lysis buffer at 4 d post-infection (dpi) and 8 dpi, respectively. The total genomic DNA from 25 mg of tissues in 100 μL of lysis buffer was extracted using the Animal Tissues/Cells Genomic DNA Extraction Kit (Solarbio, China). To draw the standard curve, genomic DNA samples of *T. gondii* were 10-fold-diluted ranging from 100 to 1×10^{-7} ng, and were then subjected to a real-time polymerase chain reaction (PCR) assay using specific primers on the CFX Manager™ Real-time System (Bio-Rad, USA). The threshold cycle (C_T) values were then calculated for these standard curves. Each sample was amplified in final volumes of 25 μL containing 12.5 μL of KOD SYBR® qPCR Mix (Toyobo, Japan), 2 μL of template DNA, 8.5 μL of distilled water, and 1 μL of the forward primer (5'-CGC TGC AGG GAG GAA GAC GAA AGT TG-3') and reverse primer (5'-CGC TGC AGA CAC AGT GCA TCT GGA TT-3'). Amplification was accomplished under the following conditions: 95 ℃ for 15 min (initial step), 40 cycles at 95 ℃ for 15 s (denaturation step), 60 ℃ for 15 s (annealing step), and 72 ℃ for 15 s (amplification step). Tachyzoites collected in ascites were counted microscopically using a hemocytometer.

2.9 Pathological analysis of liver tissues

Liver specimens from all the groups were separated and fixed in 10% (volume fraction) neutral buffered formalin for 72 h. After being embedded in paraffin, 5-μm thick tissue sections were obtained and processed for hematoxylin and eosin (H&E) staining as previously reported (Chan, 2014). The tissue sections were examined under light microscopy, with three samples selected from each group.

2.10 Flow cytometry analysis of T cell subsets

Flow cytometry was used to analyze the subsets of T cells separated from the spleens as described previously (Liu et al., 2014). Briefly, a total of 1×10^6 spleen cells were separated and collected from each mouse and incubated with anti-mouse fluorescein isothiocyanate (FITC)-cluster of differentiation 3 (CD3), allophycocyanin (APC)-cyanine dye (Cy7)-CD4, and phycoerythrin (PE)-CD8 antibodies (BD Biosciences, USA) for 15 min in the dark. After centrifugation for 2 min at 5000*g*, the supernatant was discarded, and the precipitate was resuspended with 500 μL of PBS solution. The harvested mouse spleen cells were detected on an FACSCelesta™ multicolor Flow Cytometer (BD Biosciences). The results were analyzed by FlowJo 7.6.1 software (FlowJo LLC, Ashland, OR, USA).

2.11 Cytokine detection

Briefly, a total of 50 μL serum was co-incubated with beads and with fluorescent antibodies (BD Biosciences), separately, for 2 h. Peripheral blood cytokines (interleukin-2 (IL-2), IL-4, IL-10, IL-12, and interferon-γ (IFN-γ)) were detected using BD™ Cytometric Bead Array (CBA) Kit (BD Biosciences). The results were analyzed by FlowJo 7.6.1 software (FlowJo LLC).

2.12 Statistical analysis

Statistical analyses and graphs were performed using SPSS version 26 (IBM Corporation, USA) and

GraphPad Prism 8.0 software (GraphPad Software, Inc., USA). One-way analysis of variance (ANOVA) was used to analyze statistical differences between the test and control groups with a 95% confidence interval (CI), and the Bonferroni/Tukey test was used as a post hoc test for multiple comparisons. The TC_{50} and IC_{50} values were derived from non-linear regression analysis (curve fitting). The Kaplan-Meier method was used to compare survival analysis among groups, and differences with a *P*-value of <0.05 were considered statistically significant.

3 Results

3.1 In vitro assessment of BAI and BC cytotoxicity

The cytotoxicity of BAI and BC in HFF cells was evaluated by observing cell proliferation in vitro. The results of cell proliferation measured by the CCK-8 reagent indicated that both BAI and BC had no significant toxic effect on cell growth when the concentration of BAI was ≤400 μmol/L and that of BC was ≤200 μmol/L (Fig. 1b). Additionally, both BAI and BC inhibited HFF cell growth in a dose-dependent manner, and their TC_{50} values were 592.9 and 203.7 μmol/L, respectively (Fig. 1c). Furthermore, to evaluate the anti-*T. gondii* effects of BC and BAI, HFF cell monolayers infected with *T. gondii* were treated with gradient concentrations of BC and BAI within the safe dose range. The results showed that BAI could inhibit intracellular proliferation of RH tachyzoites in a concentration-dependent manner with an IC_{50} of 64.57 μmol/L (95% CI, 48.95 to 86.15 μmol/L) (Fig. 2a), while BC did not show significant inhibition of intracellular proliferation of RH tachyzoites within the safe dose range (Fig. 2b).

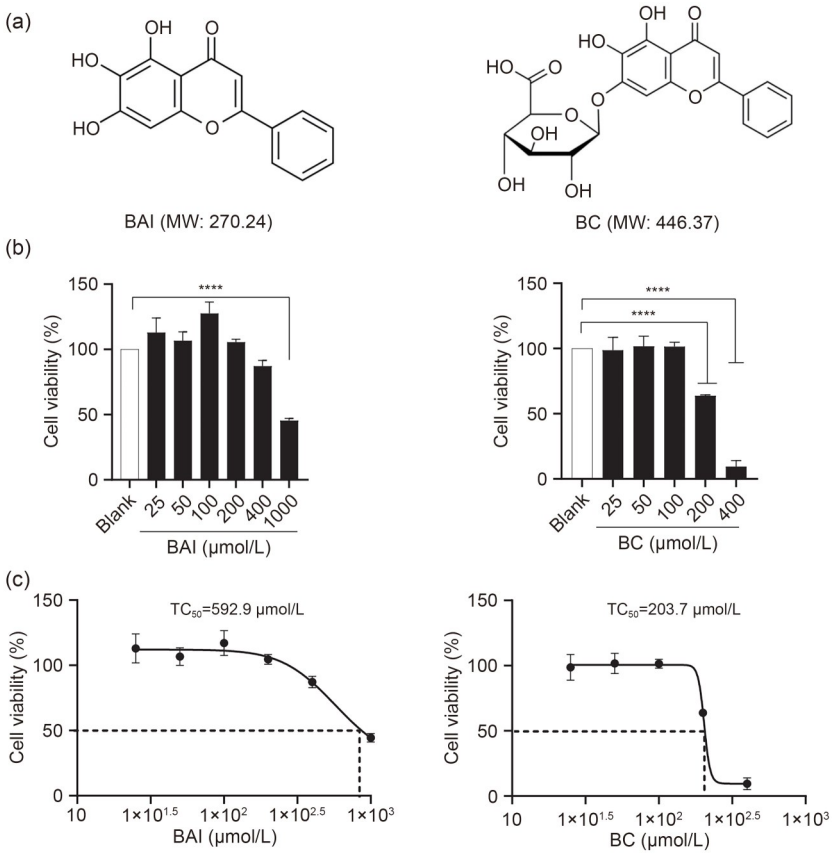

Fig. 1 Determination of the cytotoxicity of baicalein (BAI) and baicalin (BC) on human foreskin fibroblast (HFF) cells using a cell counting kit-8 (CCK-8) kit. (a) Molecular structures and molecular weights (MWs) of BAI and BC. (b) Dose–response curves and the half-maximum toxicity concentration (TC_{50}) values for BAI and BC. (c) HFF cells were treated with gradient concentrations of BAI (25, 50, 100, 200, 400, and 1000 μmol/L) or BC (25, 50, 100, 200, and 400 μmol/L) to evaluate the cytotoxicity of BAI or BC. Results are shown as the percentage of live cells relative to the blank control. The mean±standard deviation (SD) from one experiment representative of three independent experiments is shown. ** *P*<0.0001.**

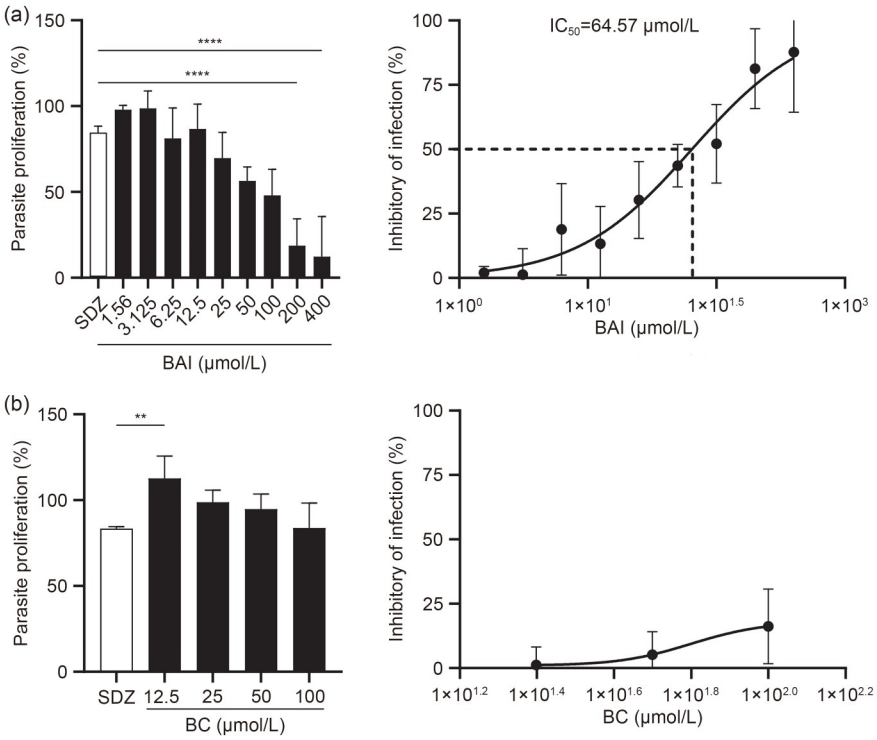

Fig. 2 Effects of baicalein (BAI) and baicalin (BC) on *Toxoplasma gondii* proliferation evaluated in human foreskin fibroblast (HFF) cells. HFF cells cultured in 96-well plates were invaded with 5×10^4 Rockefeller hospital (RH) tachyzoites per well. Infected cells were treated with 400 μmol/L sulfadiazine (SDZ). (a) Parasite proliferation in HFF cells treated with BAI of 1.56, 3.125, 6.25, 12.5, 25, 50, 100, 200, and 400 μmol/L, and the half-maximum inhibitory concentration (IC_{50}) value for BAI. (b) Parasite proliferation in HFF cells treated with BC of 12.5, 25, 50, and 100 μmol/L, and the IC_{50} value for BC. The mean±standard deviation (SD) from one experiment representative of five independent experiments is shown. ** P<0.01, **** P<0.0001.

3.2 In vitro anti-*T. gondii* efficacy of BAI

A plaque assay was performed to further validate the efficiency of BAI against *T. gondii* tachyzoites. Host HFF cells were incubated with RH tachyzoites for 7 d and then stained with crystal violet. The results showed that the plaque areas in the BAI and SDZ groups were approximately 3.71% and 5.65% of the total area, respectively, which were significantly reduced when compared with the NC group (21.50%) (Fig. 3).

To investigate the impact of BAI on the replication cycles of *T. gondii*, an indirect immunofluorescence assay (IFA) was performed to analyze the invasion efficiency and intracellular proliferation rate in HFF cells. The invasion rates of *T. gondii* treated with BAI or SDZ were 33.56% and 69.51%, respectively, and that of the NC was 66.81% (Fig. 4). The results of the invasion assay revealed that BAI treatment significantly reduced the invasion of *T. gondii*, compared with the SDZ-positive control and NC (P<0.0001).

Subsequently, the intracellular proliferation rate was calculated by counting the number of tachyzoites in at least 100 parasitophorous vacuoles (PVs). The tachyzoite numbers of the BAI and SDZ groups, with most PVs containing 1 or 2 tachyzoites, were notably lower than that of the NC group (Figs. 5a–5c). Meanwhile, the intracellular proliferation of the BAI group also showed a significantly reduced rate compared with the NC group (P<0.0001) (Fig. 5d), indicating an effective anti-*T. gondii* intracellular proliferation effect of BAI.

3.3 In vivo anti-*T. gondii* efficacy of BAI

To further investigate the therapeutic effect of BAI, mice infected with *T. gondii* were administered drugs i.g. The results of survival tests showed that mice in the NC group could survive for only 7–8 dpi, while mice in the BH, BM, and SDZ-positive groups survived for at least 24 dpi (Fig. 6a). The numbers of tachyzoites in the ascite fluid were counted microscopically

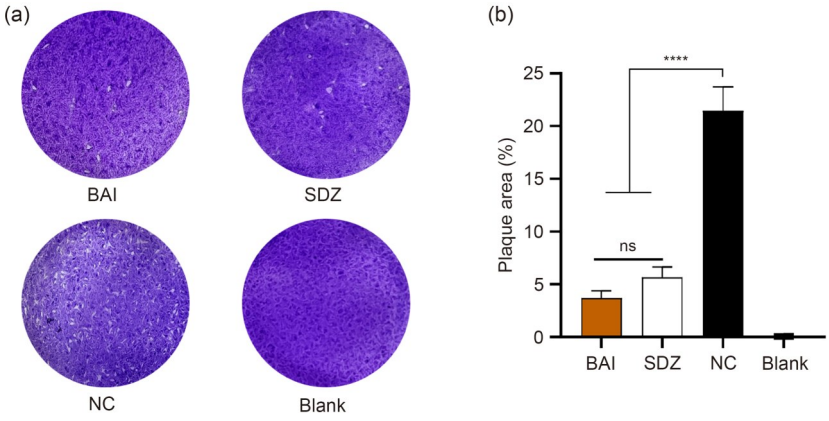

Fig. 3 Plaque assay evaluation of Rockefeller hospital (RH) tachyzoite proliferation. (a) Human foreskin fibroblast (HFF) monolayers were infected with 500 tachyzoites in a 6-well plate containing baicalein (BAI, 65 μmol/L) or sulfadiazine (SDZ, 400 μmol/L) for 7 d and stained with 1.5% crystalline violet. HFF monolayers infected with only 500 tachyzoites were regarded as the negative control (NC), and HFF cells without any treatment were regarded as the blank control. (b) The area of each well was about 9.6 cm^2, and the percentage of empty spot area was calculated. The mean± standard deviation (SD) from one experiment representative of five independent experiments is shown. ** *P*<0.0001; ns: not significant.**

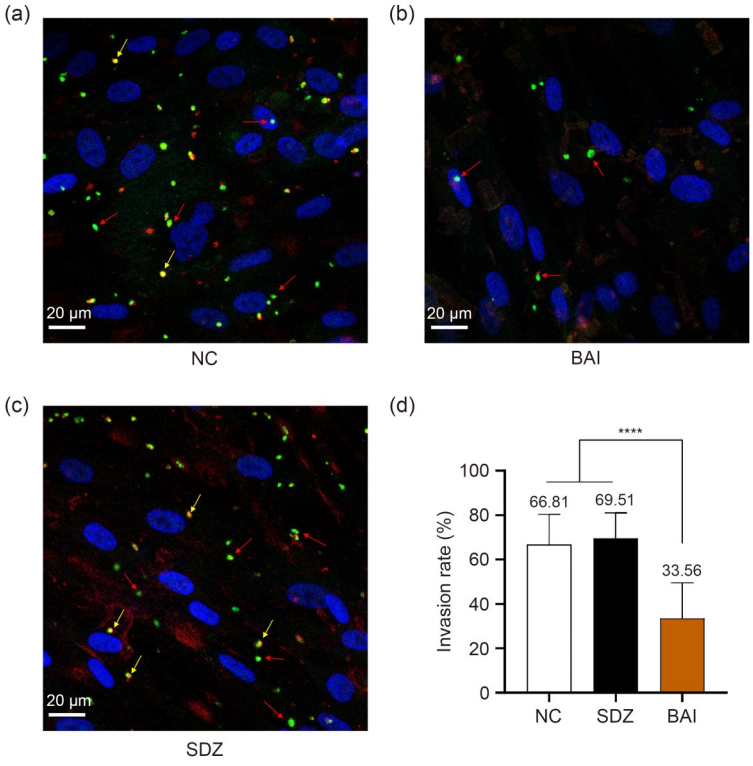

Fig. 4 Effect of baicalein (BAI) on *Toxoplasma gondii* evaluated by invasion assay. Human foreskin fibroblast (HFF) cells treated with 65 μmol/L of BAI and 400 μmol/L of sulfadiazine (SDZ) were infected with 1×10^7 Rockefeller hospital (RH) tachyzoites, and an indirect immunofluorescence assay (IFA) was performed to observe the invasion of RH tachyzoites. HFF monolayers infected with only 500 tachyzoites were used as the negative control (NC). The cells were incubated with a mouse anti-EPA45 antibody and a rabbit anti-*T. gondii* granule antigen 7 (GRA7) antibody (1:100). Goat anti-mouse Alexa Fluor 647 antibody (1:1000) and goat anti-rabbit Alexa Fluor 488 antibody (1:1000) were used as the secondary antibodies for incubation. Arrows indicate tachyzoites inside (green) or outside (yellow) host cells. (a) IFA image of the NC group. (b) IFA image of the BAI group. (c) IFA image of the SDZ group. (d) The invasion rates of *T. gondii* tachyzoites treated with BAI and SDZ were 33.56% and 69.51%, respectively, and the infected control was 66.81%. The mean± standard deviation (SD) from one experiment representative of three independent experiments is shown. ** *P*<0.0001.**

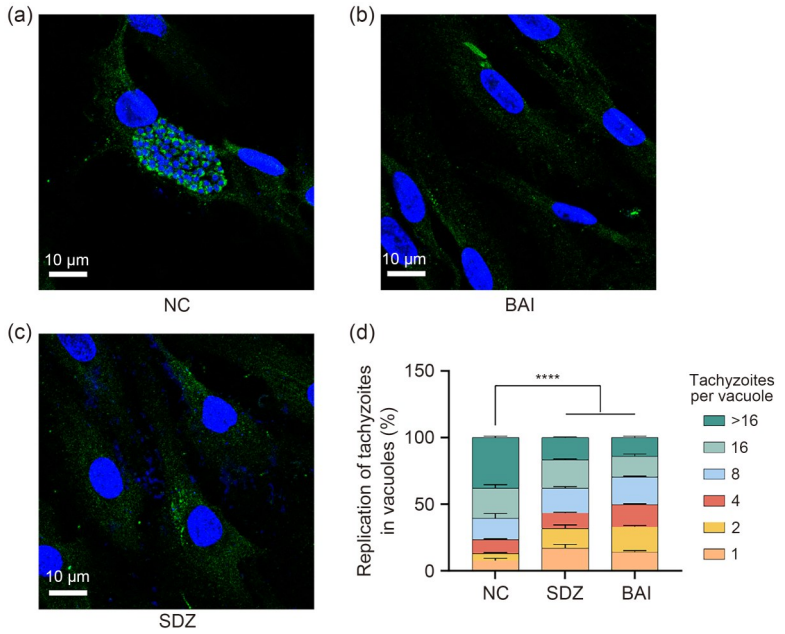

Fig. 5 Effect of baicalein (BAI) on *Toxoplasma gondii* evaluated by intracellular proliferation assay. Human foreskin fibroblast (HFF) cells treated with 65 μmol/L of BAI or 400 μmol/L of sulfadiazine (SDZ) were infected with 1×10^6 Rockefeller hospital (RH) tachyzoites, and an indirect immunofluorescence assay (IFA) was performed to mark the tachyzoites. HFF monolayers infected with only 500 tachyzoites were regarded as the negative control (NC). Cells were incubated with rabbit anti-*T. gondii* granule antigen 7 (GRA7) antibody (1:100), followed by goat anti-rabbit Alexa Fluor 488 antibody (1:1000). Green staining indicates *T. gondii* tachyzoites. (a) IFA image of the NC group. (b) IFA image of the BAI group. (c) IFA image of the SDZ group. (d) Replication of tachyzoites within cells was observed by counting at least 100 vacuoles using fluorescence microscopy and categorizing them as 1, 2, 4, 8, 16, or >16. Data (mean±SD) were analyzed using the two-way analysis of variance (ANOVA) method with three independent replicates for each count. **** $P<0.0001$.

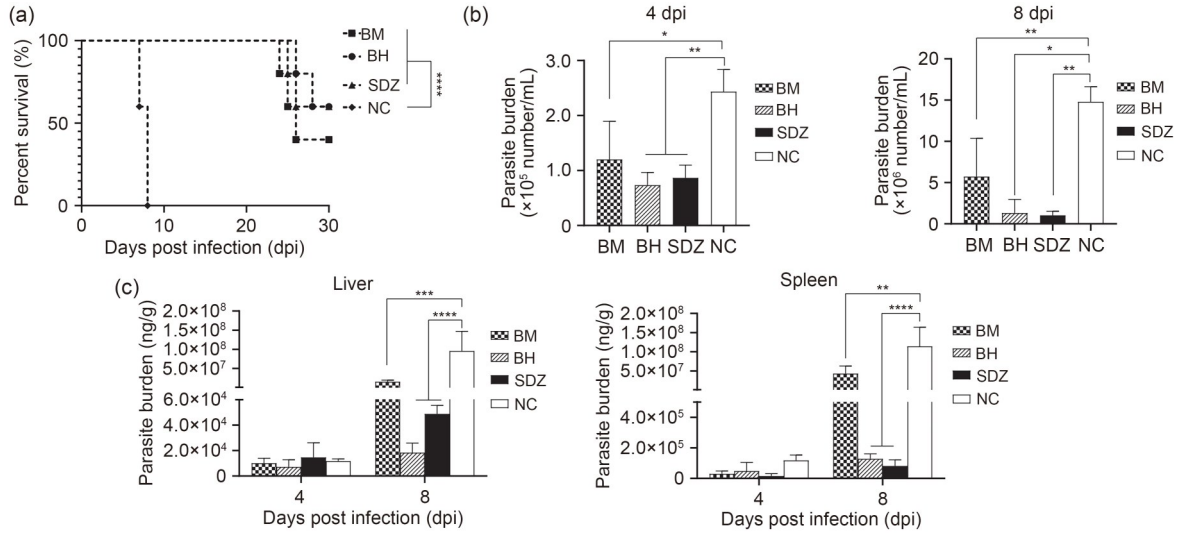

Fig. 6 Therapeutic effect of baicalein (BAI) on *Toxoplasma gondii*-infected mice. (a) ICR mice were injected with 1×10^3 Rockefeller hospital (RH) strain tachyzoites and treated with BAI (BH, 100 mg/(kg·d); BM, 100 mg/(kg·d)) and sulfadiazine (SDZ, 100 mg/(kg·d)) for 14 d, and they were observed 30 d after infection. ICR mice infected only with RH strain tachyzoites were regarded as the negative control (NC). Statistical analysis was performed using survival curves of GraphPad Prism using the log-rank (Mantel-Cox) test. (b) Tachyzoites were collected from the peritoneal cavity of the mice to determine the proliferation level of tachyzoites at 4 and 8 days post-infection (dpi), with three independent replicates for each count. (c) Quantitative polymerase chain reaction (qPCR) detection of *T. gondii* in the liver and spleen of mice. Data (mean±SD) were analyzed by GraphPad Prism 8 (GraphPad Software Inc., CA, USA) with three independent replicates for each count. * $P<0.05$, ** $P<0.01$, *** $P<0.001$, **** $P<0.0001$.

at 4 and 8 dpi. The numbers of tachyzoites were 1.2×10^5, 7.3×10^4, and 8.6×10^4 mL^{-1} in the BM, BH, and SDZ groups, respectively, which were much lower than that in the NC group (2.4×10^5 mL^{-1}) at 4 dpi (Fig. 6b). Furthermore, tachyzoite counts in the BM, BH, SDZ, and NC groups were approximately 5.7×10^6, 1.3×10^6, 1.0×10^6 and 1.5×10^7 mL^{-1}, respectively. All groups showed increased parasite loads at 8 dpi compared with those at 4 dpi, except for the BH group (Fig. 6b).

A similar tendency was observed for the number of tachyzoites in the liver and spleen at 8 dpi. In the liver, parasite burdens for the BM, BH, SDZ, and NC groups were 1.5×10^7, 1.8×10^4, 2.0×10^5, and 9.5×10^7 ng/g. In the spleen, the corresponding burdens were 4.3×10^7, 1.2×10^5, 8.2×10^4, and 1.1×10^8 ng/g (Fig. 6c). These results indicated significant reductions of parasite burden in the BH, BM, and SDZ-positive groups compared to the NC group ($P<0.0001$, $P<0.01$, $P<0.0001$, respectively).

3.4 Protective effects of BAI on liver and spleen tissues in mice

As described above, BAI was proven to significantly prolong the survival time of mice against *T. gondii* infection. A further pathological study was carried out to evaluate the protection of the liver, which is the main organ in which the parasite persists. Liver sections of mice from all groups were analyzed by performing H&E staining to determine the presence of inflammatory foci or damage. No significant inflammatory foci were observed in the BH group or the SDZ-positive control, while only mild inflammation was observed in the BM group compared with severe inflammation in the NC group (Fig. 7), indicating protection of the liver by BAI. In addition, there

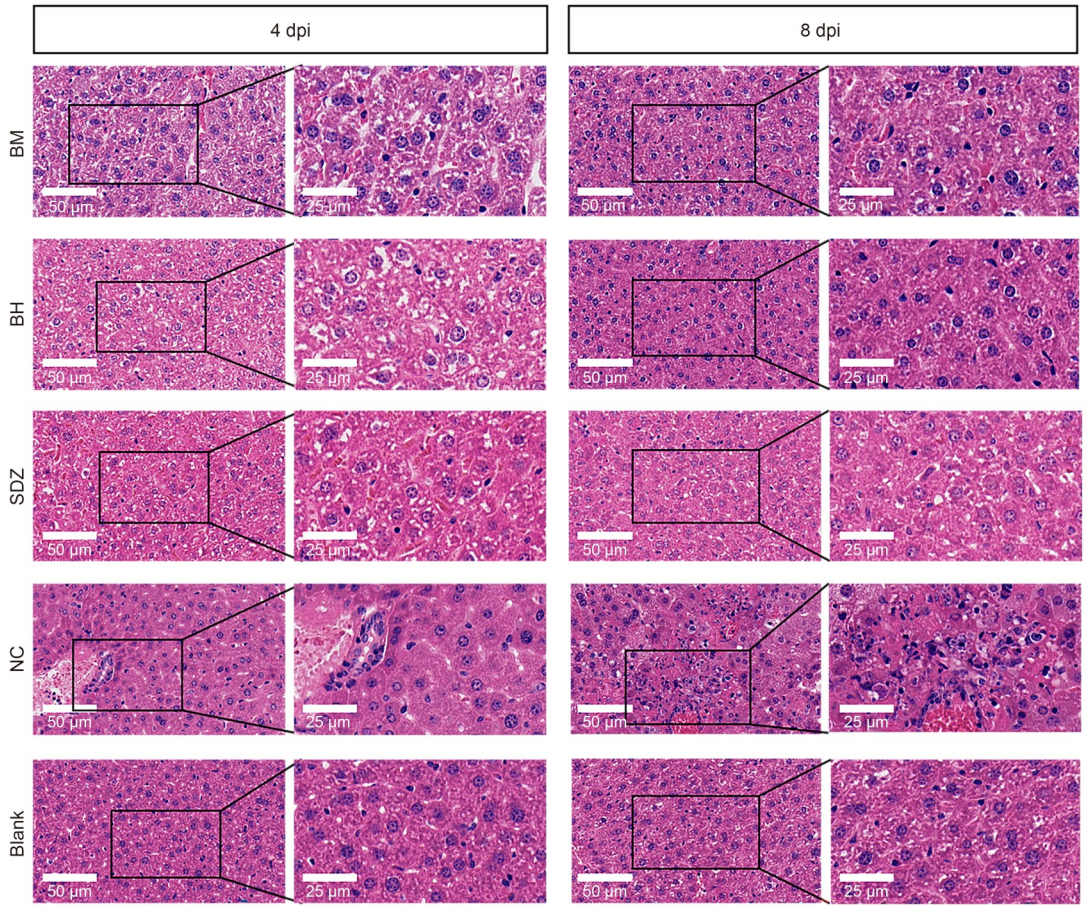

Fig. 7 Pathology of liver sections analyzed by hematoxylin and eosin (H&E) staining. Liver specimens from all the groups were separated and fixed in 10% neutral buffered formalin for 72 h. After embedding in paraffin, 5-μm thick tissue sections were obtained and processed for H&E. BM: medium-dose baicalein; BH: high-dose baicalein; SDZ: sulfadiazine; NC: phosphate-buffered saline (PBS) solution treatment; Blank: without any treatment; dpi: days post-infection.

was a significant increase in both the NC and BM groups at 8 dpi.

3.5 Effects of BAI on immune responses of *T. gondii*-infected mice

To further analyze the changes in the immune responses of BAI to *T. gondii* infection in mice, changes in T cells ($CD4^+/CD8^+$) were examined by flow cytometry. Mouse T cells were labeled with fluorescent antibodies for CD3, CD4, and CD8 to carry out the subset analyses. The results indicated that the total number of T cells increased at 4 dpi and decreased at 8 dpi in all groups. The $CD4^+/CD8^+$ ratios of the BH and NC groups increased at 4 dpi and decreased significantly at 8 dpi, but the SDZ-positive group showed no difference at the two time points. Moreover, the $CD4^+$ cell ratios changed more obviously whereas $CD8^+$ remained relatively stable (Fig. S1).

Cytokines in peripheral blood from mice infected with *T. gondii* were also detected by flow cytometry. The results showed no significant differences in IL-2 levels among groups except for the BM group, although fluctuations were observed. Notably, in the BH group, the level of IL-4 increased to 20.51 pg/mL at 4 dpi and then returned to a normal level at 8 dpi (Figs. 8a and 8b). IL-10 levels in each group were also within the normal range, but increased to 53.84 pg/mL at 8 dpi in the NC (Fig. 8b). The IL-12 levels increased substantially in all groups except for the SDZ-positive control at 4 dpi (Fig. 8a), but recovered to the low range at 8 dpi (Fig. 8b). Flow cytometry analysis of serum cytokines showed that the IFN-γ concentration of the NC increased dramatically from 4 dpi (1986.7 pg/mL) to 8 dpi (14 747.1 pg/mL) but remained at a lower level in all the drug-treated groups (Fig. 8).

4 Discussion

Toxoplasmosis, a globally prevalent zoonotic disease, poses a significant threat to immunocompromised individuals, leading to severe clinical manifestations (Du et al., 2022). Therapeutic agents for *T. gondii* infection typically involve combinations of pyrimethamine and sulphadiazine, which are always associated with adverse effects (Ben-Harari et al., 2017). In recent years, BAI and BC, flavones originally isolated from the roots of *S. baicalensis*, have exhibited potent anti-parasitic properties (Li-Weber, 2009; Johari

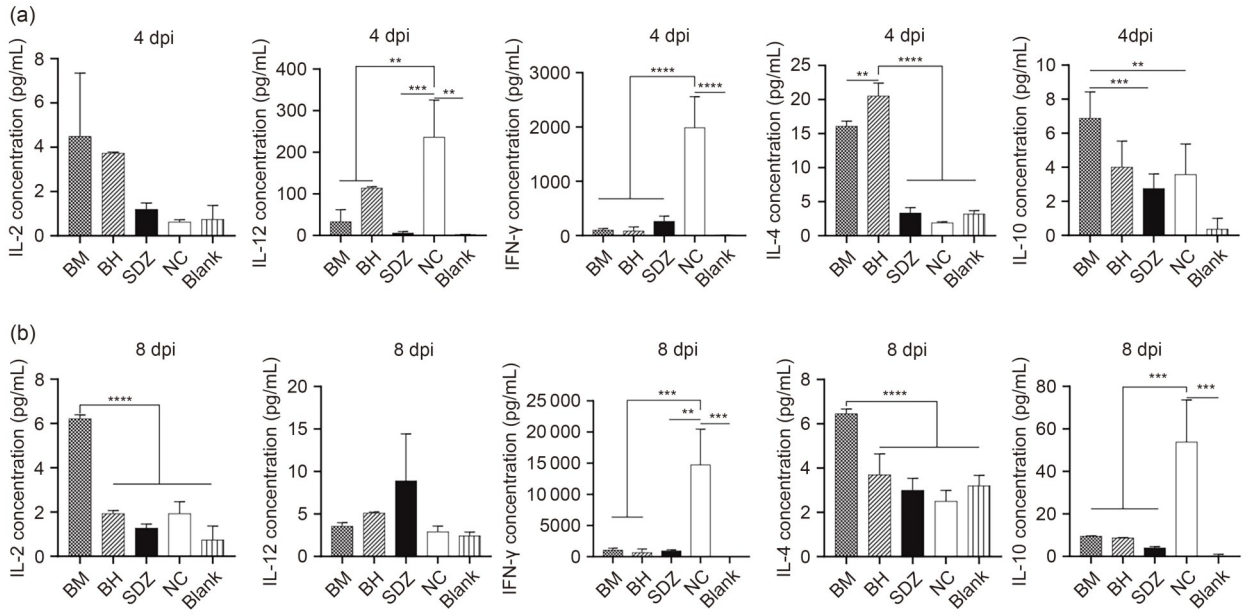

Fig. 8 Flow cytometry analyses for serum cytokines (interleukin-2 (IL-2), IL-4, IL-10, IL-12, and interferon-γ (IFN-γ)). Peripheral blood cytokines (IL-2, IL-4, IL-10, IL-12, and IFN-γ) were detected by the BD™ Cytometric Bead Array (CBA) Kit at 4 dpi (a) and 8 dpi (b). Data (mean±SD) were analyzed by GraphPad Prism 8 (GraphPad Software Inc, CA, USA) with three independent replicates for each count. ** $P<0.01$, *** $P<0.001$, **** $P<0.0001$. BM: medium-dose baicalein; BH: high-dose baicalein; SDZ: sulfadiazine; NC: phosphate-buffered saline (PBS) solution treatment; Blank: without any treatment; dpi: days post-infection.

et al., 2012; Wang et al., 2015; Luo et al., 2020). Notably, BAI has shown significant potential as a therapeutic agent against toxoplasmosis (Saito et al., 2020), leishmania (Das et al., 2006), and cryptosporidium (Jin et al., 2019; Lu et al., 2022). However, most research on the effects of BAI and BC against *T. gondii* has been confined to in vitro analyses (Yang et al., 2012; Saito et al., 2020). Therefore, we investigated the anti-*T. gondii* activity of BAI and BC by conducting a preliminary exploration of their possible use and mechanisms of action against *T. gondii*, both in vivo and in vitro.

Efficacy and cellular toxicity are the main parameters assessed in evaluating the performance of BAI. Therefore, we prioritized the assessment of its efficacy and cellular toxicity and determined the TC_{50} values for BAI and BC in HFF cells to be 592.9 and 203.7 μmol/L, respectively. Additionally, the cellular toxicity of these drugs exhibited a dose-dependent manner, indicating limited toxic effects. The corresponding therapeutic index of BAI against *T. gondii*, calculated as the ratio of TC_{50} to IC_{50} ($TI=TC_{50}/IC_{50}$), was 9.18, indicating a favorable index and a broad therapeutic window. However, the performance of BAI in our study showed both similarities and differences in terms of IC_{50} and TC_{50} compared to the study by Saito et al. (2020), which reported an IC_{50} of BAI against *T. gondii* of 5 μmol/L and a TC_{50} for HFF cells greater than 50 μmol/L.

We hypothesized that the different methodologies used for detection were mainly responsible for these differences. Saito et al. (2020) studied the direct proliferation of *T. gondii* by using a β-galactosidase reporter parasite approach, whereas our analysis relied on kits for assessing cell proliferation through a general indirect metabolic blockage method. This indirect method requires the reagents to cross host cells and parasitic vesicles before reaching the parasite, and may suffer from low sensitivity. BC did not demonstrate a significant inhibitory effect on *T. gondii* proliferation within the safe dosage range. Similar results have been observed in the later stages of the Zika virus replication cycle, indicating that BAI exhibits more significant antiviral activity than BC (Reslan et al., 2021). Previous research has also demonstrated that BAI has higher absorption and utilization rates in organisms than BC, as well as superior biological metabolic activity (de Oliveira et al., 2015). Therefore, subsequent experiments were conducted to investigate the anti-*T. gondii* properties of only BAI.

The cell viability of HFF cells was enhanced after treatment with low concentrations (from 25 to 200 μmol/L) of BAI. This phenomenon might be related to BAI-dependent protection of the cellular membrane via the redox pathway. BAI treatment can reduce the high level of reactive oxygen species (ROS) caused by hydrogen peroxide (H_2O_2) treatment and reduce the B-cell lymphoma 2 (Bcl-2) family proteins through inhibition of mitogen-activated protein kinase kinase-4 (MKK4, also known as SEK1) and c-Jun N-terminal kinase (JNK) cascades (He et al., 2009; Lee et al., 2011).

BAI significantly reduced both the invasion rate and proliferation rate of RH tachyzoites, as determined by the plaque, invasion, and intracellular proliferation assays. These assays represent the direct therapeutic effects against *T. gondii*. The results further clarified BAI's excellent intracellular inhibition of *T. gondii* reproduction and invasion. The SDZ treatment exhibited excellent intracellular inhibition of *T. gondii* reproduction, but did not show the same level of invasion as BAI. The different performance of BAI and SDZ in the invasion assay suggested that their pharmacological mechanisms might be different. SDZ primarily blocked tetrahydrofolate synthesis through competitive inhibition of dihydropteroate synthase (DHPS), which ultimately affects thymidylate synthesis in *T. gondii* (Hopper et al., 2019). In contrast, BAI was previously reported as a DNA topoisomerase inhibitor (Das et al., 2006) and could inhibit nuclear factor-κB (NF-κB) and anti-ROS activation (Qi et al., 2013; He et al., 2015; Patwardhan et al., 2016; Luo et al., 2020; Dai et al., 2021).

Based on the findings from in vitro experiments, we investigated whether BAI could effectively combat *T. gondii* infection in vivo. Mice treated with BAI or SDZ survived for 15 d, and some survived to the end of the experiment (30 dpi). Mice in the NC group survived for only 7–8 d (Fig. 6a). Infected mice treated with the combination of sulfadiazine and pyrimethamine have been shown to survive for 14–20 d (Piketty et al., 1990; Romand et al., 1993; de Oliveira et al., 2009). There are reports indicating that mice infected with *T. gondii* and treated with sulfadiazine can survive even longer than 30 d (Trinchieri, 1997). The number of tachyzoites in the ascite fluids of infected

mice in the BH group was lower than that in the SDZ group at 4 dpi and showed a significant reduction compared to the NC group (Fig. 6b). This result indicated that BAI could be a therapeutic agent with low toxicity and few adverse effects for *T. gondii* infection. Parasite burden in the liver and spleen of infected mice treated with BH and BM also exhibited the same reduction compared to the NC (Fig. 6c). Significant reduction in the number of tachyzoites could also directly slow down the progression of the infection (Lagal et al., 2015). Similarly, histological examination of the liver revealed that the BAI treatment effectively protected the hepatic tissue from damage induced by *T. gondii* infection. These results suggested that BAI directly kills *T. gondii* and effectively limits the excessive inflammatory response in the liver and spleen of *T. gondii*-infected mice. *T. gondii* without treatment reproduced rapidly and unrestrictedly, usually causing excessive inflammatory response and liver damage which can lead to death in mice in the early stages of infection (Melchor and Ewald, 2019). Liver damage, inflammation, and T lymphocytes are interconnected in a complex manner within the hepatic environment. T lymphocytes, particularly $CD4^+$ and $CD8^+$ T cells, play a crucial role in the immune response to liver injury. These T cells can differentiate into subsets that either promote (T helper 1 (Th1) and Th17) or suppress (regulatory T (Treg)) inflammation (Muscate et al., 2021). Innate-like T cells, such as natural killer T (NKT) and mucosal-associated invariant T (MAIT) cells, are abundant in the liver and have both innate and adaptive immune properties. They can rapidly produce cytokines in response to liver damage or infection, contributing to the inflammatory process and influencing liver homeostasis and disease progression (Papanastasatou and Verykokakis, 2023).

We evaluated the levels of $CD4^+$ and $CD8^+$ T cells and cytokines in serum. In general, mice treated with BAI maintained a relatively regular level of immune response compared to those in the NC group. The results showed that high and time-dependent expression of IFN-γ occurred in the serum of mice in the NC. At the same time, the IL-12 concentration in the serum of the NC peaked at 4 dpi and then returned to normal at 8 dpi (Fig. 8). It is reported that an increase in IFN-γ can limit *T. gondii* growth (Platanias, 2005; Gay et al., 2016; Olias et al., 2016). During the initial infection of mice, innate immune cells trigger IL-12 production (Trinchieri, 1997; Tomura et al., 1999). Previous studies have shown that $CD8\alpha^+$ dendritic cells release IL-12 mediated by the myeloid differentiation primary response protein 88 (MyD88), which recruits and activates NK cells to secrete IFN-γ during early immunity after infection in mice (Yarovinsky, 2008; Egan et al., 2009; Biswas et al., 2017). This was consistent with our observations. Furthermore, an increase in IL-10 was observed in the NC at 8 dpi. As IL-10 is also as known as an anti-inflammation cytokine, its elevation might be associated with an excessive, uncontrolled inflammatory response in the mice of the NC. This outcome was corroborated by the survival curve of the NC, which exhibited survival up to only 8 d. This truncated survival period might be attributable to an excessive inflammatory response. Several studies have shown that mice deficient in IL-10 or treated with anti-IL-10 neutralizing antibodies are susceptible to excessive inflammation (Neyer et al., 1997; Swierczynski et al., 2000; Hall et al., 2012).

IFN-γ is known as a crucial cytokine in the suppression of *T. gondii* tachyzoites, with its serum concentration typically rising in response to *T. gondii* infection. However, our results indicated the expression levels of IFN-γ in the SDZ and BAI groups were much lower than that observed in the NC. While there was a modest increase in IL-12 in the BH group but not in the SDZ-positive control, the levels of IL-2, IL-4, and IFN-γ did not exhibit any significant change in the SDZ group compared to those in normal mice. Furthermore, a remarkable reduction in tachyzoite proliferation was noted in the BAI and SDZ groups (Figs. 6b and 6c). These observations implied that BAI and SDZ might have the potential to directly inhibit the invasion and proliferation of tachyzoites, as supported by the results of the invasion and proliferation assays.

As mentioned above, in contrast to the SDZ group, which showed no changes in any cytokines, the BAI group exhibited slight increases of IL-4 and IL-10 compared with the blank group. As a Th2-secreted cytokine with multiple actions, IL-4 has been shown to inhibit IFN-γ production and induce proliferation of thymic T cells ($CD4^+$/$CD8^+$) (le Gros et al., 1990; Hou et al., 1994). Consistent with this, a marked increase in IL-4 serum levels was detected in the BH group at 4 dpi (Fig. 8). These observations might imply that BAI induced a mild Th1 inflammatory response while rapidly triggering a Th2 response, which

is typically associated with anti-inflammatory effects. Moreover, BAI might be capable of modulating the immune system. BAI exhibits anti-inflammatory activity in non-infectious diseases, such as autoimmune encephalomyelitis. For instance, Zeng et al. (2007) reported that BAI increased IL-4 and decreased IFN-γ in experimental autoimmune encephalomyelitis, compared with the control group. Besides, some research on infectious diseases has also shown that BAI can increase anti-inflammatory cytokines. Park et al. (2024) indicated that BAI significantly alleviated the progression of endometriosis in mouse models and increased the expression of anti-inflammatory factors, such as IL-4 receptor (IL-4R) in endometriotic lesions. IL-4 can stimulate the production of the anti-inflammatory cytokine IL-10 through the IL-4R signaling pathway (Mitchell et al., 2017), a phenomenon that we also observed in our results. Therefore, the upregulated expression of IL-4 and IL-10 in the mouse model of *T. gondii* infection appeared to be due to the role of BAI in modulating the immune system. With BAI's modulation, the expression of all cytokines returned to normal levels in the BH group at 8 dpi. As reported by Dimier-Poisson et al. (2003), an appropriate immunosuppressive response plays an important role in fighting infection with *T. gondii*. The parasite burdens were well controlled in the BH group at 8 dpi (Fig. 6b). Meanwhile, the numbers of tachyzoites in the ascites of mice within the BH group decreased from 4 to 8 dpi (Fig. 6c). Similarly, the numbers of $CD3^+CD4^+$ and $CD3^+CD8^+$ cells from mouse splenocytes showed an upward trend at 4 dpi and then a downward trend at 8 dpi, in acute infection with *T. gondii*. Notably, the T cell ratio of the BM group did not show significant variation at any time. The $CD4^+/CD8^+$ ratio changed with a similar trend caused by upregulation of $CD4^+$. The reason might be associated with the changes in cytokines described previously. As reported (Nedergaard et al., 2007; Daniel et al., 2008; Rathore et al., 2014; Luo et al., 2017), the $CD4^+/CD8^+$ ratio is often used as a monitoring indicator for tumor therapy and transplantation immunity. When the $CD4^+/CD8^+$ ratio is greater than 2, it often indicates an overwhelming immune response. However, the specific cell types of $CD4^+$ cells were still not identified (such as Th1, Th2, or Treg). This needs to be explored in further investigations of the mechanism of BAI activity against *T. gondii*.

Thus, our proposed hypothesis for BAI's anti-*T. gondii* activity is as follows: BAI might initially target topoisomerases, thereby disrupting the DNA replication and repair processes of *T. gondii*. This disruption could subsequently initiate an inflammatory cascade, characterized by the activation of NF-κB and the generation of ROS in vivo. The ability of BAI to modulate these downstream inflammatory events may be instrumental in its overall antiparasitic efficacy. Prior research has evaluated the efficacy of established topoisomerase inhibitors, such as camptothecin and 10-hydroxycamptothecin (Cristaldi et al., 2023), against *T. gondii*, providing a valuable insight into the therapeutic potential of topoisomerase inhibition as a strategy for combating this parasite.

In this study, BAI demonstrated low cytotoxicity and significant inhibitory effects against *T. gondii*, along with a broad therapeutic concentration range. Our findings suggest that its primary mechanism of action is likely associated with the attenuation of excessive inflammatory reactions and the regulation of innate immune responses. This research not only introduces a novel concept but also provides valuable insights and a foundation for further exploration in the development of traditional Chinese medicinal herbs for combating *T. gondii* infections.

Data availability statement

The authors declare that the experimental data supporting the findings of this study are available within the paper and they have no known competing financial interests or personal relationships that could influence the work presented in this paper.

Acknowledgments

This research was supported by the National Natural Science Foundation of China (No. 32370997), the Key Projects Jointly Constructed by the Ministry and the Province of Zhejiang Medical and Health Science and Technology Project (No. WKJ-ZJ-2545), the Chinese Medicine Science and Technology Program of Zhejiang Province (No. 2024ZL367), the Health Commission of Zhejiang Province (No. 2024KY923), and the Foundation of GuoTai (Taizhou) Center of Technology Innovation for Veterinary Biologicals (No. GTKF(23)001), China.

Author contributions

Songrui WU and Yingmei LAI collaborated on both the in vitro and in vivo experiments. Zhong'ao ZHANG and Jianzu DING made significant contributions to the in vivo experiments.

Songrui WU and Haojie DING played a substantial role in drafting the manuscript. Shaohong LU, Huayue YE, and Xunhui ZHUO were significantly involved in designing the experiments and revising the manuscript. All authors have read and approved the final manuscript, and therefore, have full access to all the data in the study and take responsibility for the integrity and security of the data.

Compliance with ethics guidelines

Songrui WU, Yingmei LAI, Zhong'ao ZHANG, Jianzu DING, Shaohong LU, Huayue YE, Haojie DING, and Xunhui ZHUO declare that they have no conflicts of interest.

Mice were fed in accordance with the guidelines outlined in the Guide for the Care and Use of Laboratory Animals of the Chinese Ministry of Science and Technology. The experimental procedures were approved by the Animal Experimentation Ethics Committee of Hangzhou Medical College (No. 2021-134).

References

Ben-Harari RR, Goodwin E, Casoy J, 2017. Adverse event profile of pyrimethamine-based therapy in toxoplasmosis: a systematic review. *Drugs R D*, 17(4):523-544. https://doi.org/10.1007/s40268-017-0206-8

Biswas A, French T, Düsedau HP, et al., 2017. Behavior of neutrophil granulocytes during *Toxoplasma gondii* infection in the central nervous system. *Front Cell Infect Microbiol*, 7:259. https://doi.org/10.3389/fcimb.2017.00259

Chan JKC, 2014. The wonderful colors of the hematoxylin-eosin stain in diagnostic surgical pathology. *Int J Surg Pathol*, 22(1):12-32. https://doi.org/10.1177/1066896913517939

Cheraghipour K, Masoori L, Ezzatpour B, et al., 2021. The experimental role of medicinal plants in treatment of *Toxoplasma gondii* infection: a systematic review. *Acta Parasitol*, 66(2):303-328. https://doi.org/10.1007/s11686-020-00300-4

Cristaldi C, Saldarriaga Cartagena AM, Ganuza A, et al., 2023. Evaluation of topotecan and 10-hydroxycamptothecin on *Toxoplasma gondii*: implications on baseline DNA damage and repair efficiency. *Int J Parasitol Drugs Drug Resist*, 23:120-129. https://doi.org/10.1016/j.ijpddr.2023.11.004

Daher D, Shaghlil A, Sobh E, et al., 2021. Comprehensive overview of *Toxoplasma gondii*-induced and associated diseases. *Pathogens*, 10(11):1351. https://doi.org/10.3390/pathogens10111351

Dai CS, Li H, Wang Y, et al., 2021. Inhibition of oxidative stress and ALOX12 and NF-κB pathways contribute to the protective effect of baicalein on carbon tetrachloride-induced acute liver injury. *Antioxidants (Basel)*, 10(6):976. https://doi.org/10.3390/antiox10060976

Daniel V, Naujokat C, Sadeghi M, et al., 2008. Observational support for an immunoregulatory role of $CD3^+CD4^+CD25^+IFN\text{-}\gamma^+$ blood lymphocytes in kidney transplant recipients with good long-term graft outcome. *Transpl Int*, 21(7):646-660. https://doi.org/10.1111/j.1432-2277.2008.00662.x

Das BB, Sen N, Roy A, et al., 2006. Differential induction of *Leishmania donovani* bi-subunit topoisomerase I–DNA cleavage complex by selected flavones and camptothecin: activity of flavones against camptothecin-resistant topoisomerase I. *Nucleic Acids Res*, 34(4):1121-1132. https://doi.org/10.1093/nar/gkj502

de Oliveira MR, Nabavi SF, Habtemariam S, et al., 2015. The effects of baicalein and baicalin on mitochondrial function and dynamics: a review. *Pharmacol Res*, 100:296-308. https://doi.org/10.1016/j.phrs.2015.08.021

de Oliveira TC, Oliveira Silva DA, Rostkowska C, et al., 2009. *Toxoplasma gondii*: effects of *Artemisia annua* L. on susceptibility to infection in experimental models in vitro and in vivo. *Exp Parasitol*, 122(3):233-241. https://doi.org/10.1016/j.exppara.2009.04.010

Dimier-Poisson I, Aline F, Mévélec MN, et al., 2003. Protective mucosal Th2 immune response against *Toxoplasma gondii* by murine mesenteric lymph node dendritic cells. *Infect Immun*, 71(9):5254-5265. https://doi.org/10.1128/iai.71.9.5254-5265.2003

Dinda B, Dinda S, Dassharma S, et al., 2017. Therapeutic potentials of baicalin and its aglycone, baicalein against inflammatory disorders. *Eur J Med Chem*, 131:68-80. https://doi.org/10.1016/j.ejmech.2017.03.004

Djurković-Djaković O, Milenković V, Nikolić A, et al., 2002. Efficacy of atovaquone combined with clindamycin against murine infection with a cystogenic (Me49) strain of *Toxoplasma gondii*. *J Antimicrob Chemother*, 50(6):981-987. https://doi.org/10.1093/jac/dkf251

Du KG, Lu F, Xie CZ, et al., 2022. *Toxoplasma gondii* infection induces cell apoptosis via multiple pathways revealed by transcriptome analysis. *J Zhejiang Univ-Sci B (Biomed & Biotechnol)*, 23(4):315-327. https://doi.org/10.1631/jzus.B2100877

Egan CE, Sukhumavasi W, Butcher BA, et al., 2009. Functional aspects of Toll-like receptor/MyD88 signalling during protozoan infection: focus on *Toxoplasma gondii*. *Clin Exp Immunol*, 156(1):17-24. https://doi.org/10.1111/j.1365-2249.2009.03876.x

Fichera ME, Bhopale MK, Roos DS, 1995. In vitro assays elucidate peculiar kinetics of clindamycin action against *Toxoplasma gondii*. *Antimicrob Agents Chemother*, 39(7):1530-1537. https://doi.org/10.1128/aac.39.7.1530

Fox BA, Bzik DJ, 2002. *De novo* pyrimidine biosynthesis is required for virulence of *Toxoplasma gondii*. *Nature*, 415(6874):926-929. https://doi.org/10.1038/415926a

Gay G, Braun L, Brenier-Pinchart MP, et al., 2016. *Toxoplasma gondii* TgIST co-opts host chromatin repressors dampening STAT1-dependent gene regulation and IFN-γ-mediated host defenses. *J Exp Med*, 213(9):1779-1798.

https://doi.org/10.1084/jem.20160340

Hall AO, Beiting DP, Tato C, et al., 2012. The cytokines interleukin 27 and interferon-γ promote distinct Treg cell populations required to limit infection-induced pathology. *Immunity*, 37(3):511-523. https://doi.org/10.1016/j.immuni.2012.06.014

Haverkos HW, 1987. Assessment of therapy for toxoplasma encephalitis the TE study group. *Am J Med*, 82(5):907-914. https://doi.org/10.1016/0002-9343(87)90151-3

He XL, Wang YH, Gao M, et al., 2009. Baicalein protects rat brain mitochondria against chronic cerebral hypoperfusion-induced oxidative damage. *Brain Res*, 1249:212-221. https://doi.org/10.1016/j.brainres.2008.10.005

He XX, Wei ZK, Zhou ES, et al., 2015. Baicalein attenuates inflammatory responses by suppressing TLR4 mediated NF-κB and MAPK signaling pathways in LPS-induced mastitis in mice. *Int Immunopharmacol*, 28(1):470-476. https://doi.org/10.1016/j.intimp.2015.07.012

Hopper AT, Brockman A, Wise A, et al., 2019. Discovery of selective *Toxoplasma gondii* dihydrofolate reductase inhibitors for the treatment of toxoplasmosis. *J Med Chem*, 62(3):1562-1576. https://doi.org/10.1021/acs.jmedchem.8b01754

Hou JZ, Schindler U, Henzel WJ, et al., 1994. An interleukin-4-induced transcription factor: IL-4 Stat. *Science*, 265(5179):1701-1706. https://doi.org/10.1126/science.8085155

Hu QC, Zhang WW, Wu Z, et al., 2021. Baicalin and the liver-gut system: pharmacological bases explaining its therapeutic effects. *Pharmacol Res*, 165:105444. https://doi.org/10.1016/j.phrs.2021.105444

Jiang LP, Liu B, Hou SJ, et al., 2022. Discovery and evaluation of chalcone derivatives as novel potential anti-*Toxoplasma gondii* agents. *Eur J Med Chem*, 234:114244. https://doi.org/10.1016/j.ejmech.2022.114244

Jin Z, Ma JB, Zhu G, et al., 2019. Discovery of novel anti-cryptosporidial activities from natural products by *in vitro* high-throughput phenotypic screening. *Front Microbiol*, 10:1999. https://doi.org/10.3389/fmicb.2019.01999

Johari J, Kianmehr A, Mustafa MR, et al., 2012. Antiviral activity of baicalein and quercetin against the Japanese encephalitis virus. *Int J Mol Sci*, 13(12):16785-16795. https://doi.org/10.3390/ijms131216785

Kovacs JA, 1992. Efficacy of atovaquone in treatment of toxoplasmosis in patients with AIDS. *Lancet*, 340(8820):637-638. https://doi.org/10.1016/0140-6736(92)92172-c

Lagal V, Dinis M, Cannella D, et al., 2015. AMA1-deficient *Toxoplasma gondii* parasites transiently colonize mice and trigger an innate immune response that leads to long-lasting protective immunity. *Infect Immun*, 83(6):2475-2486. https://doi.org/10.1128/iai.02606-14

le Gros G, Ben-Sasson SZ, Seder R, et al., 1990. Generation of interleukin 4 (IL-4)-producing cells in vivo and in vitro: IL-2 and IL-4 are required for in vitro generation of IL-4-producing cells. *J Exp Med*, 172(3):921-929. https://doi.org/10.1084/jem.172.3.921

Lee IK, Kang KA, Zhang R, et al., 2011. Mitochondria protection of baicalein against oxidative damage via induction of manganese superoxide dismutase. *Environ Toxicol Pharmacol*, 31(1):233-241. https://doi.org/10.1016/j.etap.2010.11.002

Li W, Grech J, Stortz JF, et al., 2022. A splitCas9 phenotypic screen in *Toxoplasma gondii* identifies proteins involved in host cell egress and invasion. *Nat Microbiol*, 7(6):882-895. https://doi.org/10.1038/s41564-022-01114-y

Li-Weber M, 2009. New therapeutic aspects of flavones: the anticancer properties of *Scutellaria* and its main active constituents Wogonin, Baicalein and Baicalin. *Cancer Treat Rev*, 35(1):57-68. https://doi.org/10.1016/j.ctrv.2008.09.005

Liang W, Huang XB, Chen WQ, 2017. The effects of baicalin and baicalein on cerebral ischemia: a review. *Aging Dis*, 8(6):850-867. https://doi.org/10.14336/ad.2017.0829

Liu G, Li ZF, Wei Y, et al., 2014. Direct detection of FoxP3 expression in thymic double-negative $CD4^{-}CD8^{-}$ cells by flow cytometry. *Sci Rep*, 4:5781. https://doi.org/10.1038/srep05781

Liu SX, Wu MM, Hua QQ, et al., 2020. Two old drugs, NVP-AEW541 and GSK-J4, repurposed against the *Toxoplasma gondii* RH strain. *Parasit Vectors*, 13:242. https://doi.org/10.1186/s13071-020-04094-2

Lu CX, Liu XY, Liu J, et al., 2022. Immunocompetent rabbits infected with *Cryptosporidium cuniculus* as an animal model for anti-cryptosporidial drug testing. *Int J Parasitol*, 52(4):205-210. https://doi.org/10.1016/j.ijpara.2021.10.006

Luo Q, Ye JQ, Zeng LL, et al., 2017. Elevated expression of TIGIT on $CD3^{+}CD4^{+}$ T cells correlates with disease activity in systemic lupus erythematosus. *Allergy Asthma Clin Immunol*, 13:15. https://doi.org/10.1186/s13223-017-0188-7

Luo Z, Kuang XP, Zhou QQ, et al., 2020. Inhibitory effects of baicalein against herpes simplex virus type 1. *Acta Pharm Sin B*, 10(12):2323-2338. https://doi.org/10.1016/j.apsb.2020.06.008

Melchor SJ, Ewald SE, 2019. Disease tolerance in *Toxoplasma* infection. *Front Cell Infect Microbiol*, 9:185. https://doi.org/10.3389/fcimb.2019.00185

Mitchell RE, Hassan M, Burton BR, et al., 2017. IL-4 enhances IL-10 production in Th1 cells: implications for Th1 and Th2 regulation. *Sci Rep*, 7:11315. https://doi.org/10.1038/s41598-017-11803-y

Montazeri M, Sharif M, Sarvi S, et al., 2017. A systematic review of *in vitro* and *in vivo* activities of anti-*Toxoplasma* drugs and compounds (2006–2016). *Front Microbiol*, 8:25. https://doi.org/10.3389/fmicb.2017.00025

Munoz M, Liesenfeld O, Heimesaat MM, 2011. Immunology of *Toxoplasma gondii*. *Immunol Rev*, 240(1):269-285. https://doi.org/10.1111/j.1600-065X.2010.00992.x

Muscate F, Woestemeier A, Gagliani N, 2021. Functional heterogeneity of $CD4^+$ T cells in liver inflammation. *Semin Immunopathol*, 43(4):549-561. https://doi.org/10.1007/s00281-021-00881-w

Nedergaard BS, Ladekarl M, Thomsen HF, et al., 2007. Low density of $CD3^+$, $CD4^+$ and $CD8^+$ cells is associated with increased risk of relapse in squamous cell cervical cancer. *Br J Cancer*, 97(8):1135-1138. https://doi.org/10.1038/sj.bjc.6604001

Neyer LE, Grunig G, Fort M, et al., 1997. Role of interleukin-10 in regulation of T-cell-dependent and T-cell-independent mechanisms of resistance to *Toxoplasma gondii*. *Infect Immun*, 65(5):1675-1682. https://doi.org/10.1128/iai.65.5.1675-1682.1997

Olias P, Etheridge RD, Zhang Y, et al., 2016. *Toxoplasma* effector recruits the Mi-2/NuRD complex to repress STAT1 transcription and block IFN-γ-dependent gene expression. *Cell Host Microbe*, 20(1):72-82. https://doi.org/10.1016/j.chom.2016.06.006

Papanastasatou M, Verykokakis M, 2023. Innate-like T lymphocytes in chronic liver disease. *Front Immunol*, 14:1114605. https://doi.org/10.3389/fimmu.2023.1114605

Park W, Jang H, Kim HS, et al., 2024. Therapeutic efficacy and anti-inflammatory mechanism of baicalein on endometriosis progression in patient-derived cell line and mouse model. *Phytomedicine*, 130:155469. https://doi.org/10.1016/j.phymed.2024.155469

Patwardhan RS, Sharma D, Thoh M, et al., 2016. Baicalein exhibits anti-inflammatory effects via inhibition of NF-κB transactivation. *Biochem Pharmacol*, 108:75-89. https://doi.org/10.1016/j.bcp.2016.03.013

Piketty C, Derouin F, Rouveix B, et al., 1990. In vivo assessment of antimicrobial agents against *Toxoplasma gondii* by quantification of parasites in the blood, lungs, and brain of infected mice. *Antimicrob Agents Chemother*, 34(8):1467-1472. https://doi.org/10.1128/aac.34.8.1467

Platanias LC, 2005. Mechanisms of type-I- and type-II-interferon-mediated signalling. *Nat Rev Immunol*, 5(5):375-386. https://doi.org/10.1038/nri1604

Porter SB, Sande MA, 1992. Toxoplasmosis of the central nervous system in the acquired immunodeficiency syndrome. *N Engl J Med*, 327(23):1643-1648. https://doi.org/10.1056/nejm199212033272306

Qi ZL, Yin F, Lu LN, et al., 2013. Baicalein reduces lipopolysaccharide-induced inflammation via suppressing JAK/STATs activation and ROS production. *Inflamm Res*, 62(9):845-855. https://doi.org/10.1007/s00011-013-0639-7

Rathore AS, Kumar S, Konwar R, et al., 2014. CD3+, CD4+ & CD8+ tumour infiltrating lymphocytes (TILs) are predictors of favourable survival outcome in infiltrating ductal carcinoma of breast. *Indian J Med Res*, 140(3):361-369.

Reslan A, Haddad JG, Moukendza Koundi L, et al., 2021. Zika virus growth in human kidney cells is restricted by an elevated glucose level. *Int J Mol Sci*, 22(5):2495. https://doi.org/10.3390/ijms22052495

Romand S, Pudney M, Derouin F, 1993. In vitro and in vivo activities of the hydroxynaphthoquinone atovaquone alone or combined with pyrimethamine, sulfadiazine, clarithromycin, or minocycline against *Toxoplasma gondii*. *Antimicrob Agents Chemother*, 37(11):2371-2378. https://doi.org/10.1128/aac.37.11.2371

Saito H, Murata Y, Nonaka M, et al., 2020. Screening of a library of traditional Chinese medicines to identify compounds and extracts which inhibit *Toxoplasma gondii* growth. *J Vet Med Sci*, 82(2):184-187. https://doi.org/10.1292/jvms.19-0241

Soheilian M, Ramezani A, Azimzadeh A, et al., 2011. Randomized trial of intravitreal clindamycin and dexamethasone versus pyrimethamine, sulfadiazine, and prednisolone in treatment of ocular toxoplasmosis. *Ophthalmology*, 118(1):134-141. https://doi.org/10.1016/j.ophtha.2010.04.020

Sowndhararajan K, Deepa P, Kim M, et al., 2017. Baicalein as a potent neuroprotective agent: a review. *Biomed Pharmacother*, 95:1021-1032. https://doi.org/10.1016/j.biopha.2017.08.135

Swierczynski B, Bessieres MH, Cassaing S, et al., 2000. Inhibitory activity of anti-interleukin-4 and anti-interleukin-10 antibodies on *Toxoplasma gondii* proliferation in mouse peritoneal macrophages cocultured with splenocytes from infected mice. *Parasitol Res*, 86(2):151-157. https://doi.org/10.1007/s004360050024

Tomura M, Yu WG, Ahn HJ, et al., 1999. A novel function of $V\alpha14^+CD4^+$NKT cells: stimulation of IL-12 production by antigen-presenting cells in the innate immune system. *J Immunol*, 163(1):93-101. https://doi.org/10.4049/jimmunol.163.1.93

Trinchieri G, 1997. Cytokines acting on or secreted by macrophages during intracellular infection (IL-10, IL-12, IFN-γ). *Curr Opin Immunol*, 9(1):17-23. https://doi.org/10.1016/s0952-7915(97)80154-9

Wang X, Xie L, Long JY, et al., 2022. Therapeutic effect of baicalin on inflammatory bowel disease: a review. *J Ethnopharmacol*, 283:114749. https://doi.org/10.1016/j.jep.2021.114749

Wang YJ, Han E, Xing QH, et al., 2015. Baicalein upregulates DDIT4 expression which mediates mTOR inhibition and growth inhibition in cancer cells. *Cancer Lett*, 358(2):170-179. https://doi.org/10.1016/j.canlet.2014.12.033

Xin LY, Gao JL, Lin HC, et al., 2020. Regulatory mechanisms of baicalin in cardiovascular diseases: a review. *Front Pharmacol*, 11:583200. https://doi.org/10.3389/fphar.2020.583200

Yang XY, Huang B, Chen JP, et al., 2012. In vitro effects of aqueous extracts of *Astragalus membranaceus* and *Scutellaria baicalensis* GEORGI on *Toxoplasma gondii*.

Parasitol Res, 110(6):2221-2227. https://doi.org/10.1007/s00436-011-2752-2

Yarovinsky F, 2008. Toll-like receptors and their role in host resistance to *Toxoplasma gondii*. *Immunol Lett*, 119(1-2): 17-21. https://doi.org/10.1016/j.imlet.2008.05.007

Yun MY, Yang JH, Kim DK, et al., 2010. Therapeutic effects of baicalein on atopic dermatitis-like skin lesions of NC/Nga mice induced by dermatophagoides pteronyssinus. *Int Immunopharmacol*, 10(9):1142-1148. https://doi.org/10.1016/j.intimp.2010.06.020

Zeng Y, Song C, Ding X, et al., 2007. Baicalin reduces the severity of experimental autoimmune encephalomyelitis. *Braz J Med Biol Res*, 40(7):1003-1010. https://doi.org/10.1590/s0100-879x2006005000115

Zhang JL, Si HF, Li B, et al., 2019. Myrislignan exhibits activities against *Toxoplasma gondii* RH strain by triggering mitochondrial dysfunction. *Front Microbiol*, 10:2152. https://doi.org/10.3389/fmicb.2019.02152

Zhao XY, Kong DW, Zhou QM, et al., 2021. Baicalein alleviates depression-like behavior in rotenone-induced Parkinson's disease model in mice through activating the BDNF/TrkB/CREB pathway. *Biomed Pharmacother*, 140: 111556. https://doi.org/10.1016/j.biopha.2021.111556

Supplementary information

Fig. S1